[5]Salzano, F. J., and Aronson, S., "Thermodynamic Properties of the Cesium-Graphite Lamellar Compounds," *Journal of Chemical Physics*, Vol. 43, No. 1, 1965, pp. 149–154.

[6]Yates, M. K., "Temperature Control and Thermal Coupling of an Integral Adsorption-Type Cesium Reservoir," *Thermionic Conversion Specialists Conference* (Houston, TX), IEEE, New York, 1966, pp. 249–258.

[7]Horner-Richardson, K. D., and Kim, K. Y., "Sorption Reservoirs for Thermionic Converters," *Ninth Symposium on Space Nuclear Power Systems* (Albuquerque, NM), American Inst. of Physics, New York, 1992, pp. 629–637.

Transient Conductive and Radiative Heat Transfer in a Silica Window

Ming-Horng Su* and William H. Sutton†
University of Oklahoma, Norman, Oklahoma 73019

Nomenclature

h	=	convective heat transfer coefficient
I	=	intensity, I^+, I^- denote positive and negative η directions, respectively
$I_{\lambda b}$	=	Planck's distribution function
L	=	thickness
n	=	refractive index
Q^c	=	dimensionless conduction heat flux, $q_i^c/h(T_{aw} - T_{\infty 1})$
Q^r	=	dimensionless net radiation heat flux, $q_i^r/h(T_{aw} - T_{\infty 1})$
q^r	=	net radiative heat flux
q_i^r	=	net radiative heat flux at node i
T	=	temperature
T_{aw}	=	adiabatic wall temperature
T_0	=	initial temperature
$T_{\infty 1}$, $T_{\infty 2}$	=	ambient temperature at the first and second boundary
t	=	time
z	=	position
α	=	thermal diffusivity, $k/\rho^* c_p$, thermal conductivity/(density × specific heat)
Δ	=	increment
η	=	dimensionless axial coordinate, z/L
Θ	=	dimensionless temperature, $T/T_{\infty 1}$
θ_{cr}	=	critical angle
θ_2	=	refracted internal polar angle
κ	=	absorption coefficient
λ	=	wavelength
ρ^*	=	density
ρ_i, ρ_o	=	reflectivity inside and outside of glass

Subscript

λ	=	wavelength dependency

Introduction

THE purpose of this study is to present solutions for the transient temperature distribution in a nongray electromagnetic window, externally heated by time-independent convective flux for high-speed flow, for a short time interval (5 s). The temperature variation within the window is important because its electromagnetic transmission characteristics are dependent upon temperature. The window is modeled as a one-dimensional slab with directional-dependent specularly reflecting surfaces described by the Fresnel relations. The convective heat transfer coefficient is specified. Several investigators have analyzed combined conductive and radiative heat transfer in a one-dimensional medium,[1,2] but with different boundary conditions or conditions than those used there.

Formulation

The governing differential transient energy equation for temperature is

$$\rho^* c_p \frac{\partial T}{\partial t} + \frac{\partial}{\partial z}\left[-k\frac{\partial T}{\partial z} + q^r\right] = 0 \qquad 0 < z < L, \quad t > 0 \tag{1}$$

The boundary conditions are

$$[h(T_{aw} - T) + q^r]_{z=0^-} = \left[-k\frac{\partial T}{\partial z} + q^r\right]_{z=0^+}, \qquad t > 0 \tag{2}$$

$$\left[-k\frac{\partial T}{\partial z} + q^r\right]_{z=L^-} = [q^r]_{z=L^+}, \qquad t > 0 \tag{3}$$

where q^r is evaluated, as noted, independently on each side of the boundary interface. The values are expected to be equal in the analytical sense, but could vary in the finite difference model. The initial condition is

$$T(z, 0) = T_0, \qquad 0 \le z \le L \tag{4}$$

The radiative transfer equation for a nongray, absorbing and emitting slab is

$$\cos\theta_2 \frac{\partial I_\lambda}{\partial z} + \kappa_\lambda I_\lambda = \kappa_\lambda I_{b\lambda}[T(z)] \qquad 0 < z < L, \quad 0 < \theta_2 < \frac{\pi}{2} \tag{5}$$

The radiative boundary conditions with specular Fresnel reflection are

$$I_\lambda^+(0, \theta_2) = (1 - \rho_o) I_{\lambda b}[T_{\infty 1}] + \rho_i I_\lambda^-(0, \theta_2) \qquad 0 < \theta_2 < \theta_{cr} \tag{6}$$

$$I_\lambda^+(0, \theta_2) = I_\lambda^-(0, \theta_2), \qquad \theta_{cr} < \theta_2 < \pi/2 \tag{7}$$

$$I_\lambda^-(L, \theta_2) = (1 - \rho_o) I_{\lambda b}[T_{\infty 2}] + \rho_i I_\lambda^+(L, \theta_2) \qquad 0 < \theta_2 < \theta_{cr} \tag{8}$$

$$I_\lambda^-(L, \theta_2) = I_\lambda^+(L, \theta_2), \qquad \theta_{cr} < \theta_2 < \pi/2 \tag{9}$$

When a beam is incident on the interface from the glass side, ρ_i may be calculated by substituting $1/n$ for n, for all θ_2 less than θ_{cr}; above this angle, the beams undergo total internal reflection and $\rho_i = 1$ so that the reflectivity from the glass side ρ_i and the reflectivity from the air side ρ_o are considerably different.

The external hemispherical solid angle is remapped through Snell's law into a smaller cone of radiation with angle θ_2 depending on nongray refractive indexes; therefore, the in-

Received Feb. 19, 1993; revision received Feb. 28, 1994; accepted for publication Feb. 28, 1994.

*Research Associate, School of Aerospace and Mechanical Engineering.

†Associate Professor, School of Aerospace and Mechanical Engineering.

ternal angle θ_2 is used throughout the computations. The resulting set of combined equations is solved numerically.

An implicit finite difference method is applied to the conduction energy equation using 101 equally spaced nodes, including boundary nodes, which were found to be sufficiently accurate to reproduce exact pure conduction results. The implicit representation has no limits on time increment Δt; however, adequate spatial resolution of temperature requires a large number of locations to evaluate the radiative interaction.[3] Also, the high apparent convective flux from T_{aw}, yields an extremely steep temperature gradient near that boundary. Details of this modeling may be found in the literature.[4] This causes the equations to be stiff, i.e., to change character so that the grid for thermal diffusion becomes inadequate for low spacial resolution. A tridiagonal solver[5] was used for the conduction nodal equations.

Silicate glasses are essentially opaque to radiation having a wavelength longer than about 4 μm, and computations assume an opaque medium in that wavelength range. The intensities in the positive direction I_λ^+ (backward differenced) and negative direction I_λ^- (forward differenced) are calculated by using a finite difference/discrete ordinates approach for the radiative transfer equation.[3] The radiative heat flux is calculated from the finite difference component of the following expression:

$$q_i' = 2\pi \int_{\lambda=0}^{\infty} \int_0^1 [I_\lambda^+(z_i, \theta_2) - I_\lambda^-(z_i, \theta_2)] \cos\theta_2 \, \mathrm{d}(\cos\theta_2) \, \mathrm{d}\lambda \tag{10}$$

The numerical method was verified against constant property transmission and reflection analysis from Siegel and Howell[6] reproducing those exact results. The difference form of the radiative transfer equation is explicit in form and only requires iteration with the boundary conditions at each selected wavelength. Once the intensity is evaluated for all wavelengths, the radiative contributions are iterated at each time step until the temperature and Planck function contributions are consistent.

Data for Optical Constants

Data for the optical constants for fused silica were obtained from several sources.[2,7,12] In general, the thermal and radiative properties vary with temperature, but refractive index and absorption coefficient also vary with wavelength. Few sources have properties for the high temperatures of interest. Malitson[11] measured the index of refraction of optical quality fused silica for wavelengths from 0.21 to 3.71 μ at 20°C. The index values were fitted to the three-term Sellmeier dispersion equation:

$$n^2 = 1 + \frac{0.6961663\lambda^2}{\lambda^2 - (0.0684043)^2} + \frac{0.4079426\lambda^2}{\lambda^2 - (0.1162414)^2} + \frac{0.8974794\lambda^2}{\lambda^2 - (9.896161)^2} \tag{11}$$

Wray and Neu[12] measured the index of refraction for fused silica in the range 0.2–3.4 μ, and at temperatures from 26 to 826°C. From the data, one can find an average temperature difference parameter, 1.1×10^{-5}, and define the refractive index as a function of both wavelength and temperature

$$n(\lambda, T) = n[\text{from Eq. (11)}] + 1.1 \times 10^{-5}(T - 293\ \text{K}) \tag{12}$$

The value of the refractive index increases as the temperature increases. The highest temperature discussed in Ref. 12 is 826°C, which is much lower than the temperature of the window in the current work. Since no other experimental data are available for higher temperature, Eq. (12) is extrapolated for this work. If absorptive index is used, the relationship may be found in the text by Modest.[13] A larger refractive index causes the θ_{cr} to decrease and more energy to be reflected internally.

The current work uses temperature-dependent absorption coefficient data for 16 discrete wave bands, evenly spaced between 1–4 μm and 18 and 1300°C from Fig. 2 of Gardon.[2] There were no significant differences in results for numerous trial cases computed by using various extrapolations beyond these limitations.

Results and Conclusions

Figure 1a shows the transient Θ as a function of η. Time varies from 0.1 to 5 s. The ambient temperatures, $T_{\infty 1}$ and $T_{\infty 2}$, are held fixed at 295 K for all figures. In Fig. 1a, a very high heat transfer coefficient [Biot number of 60, h = 4.8436 kW/(m^2·°C)] and high adiabatic wall temperature (3715 K) cause the steep temperature profile near the boundary. The temperatures near the second boundary increase little. Glass is a poor thermal conductor; it is also optically thick or opaque for certain ranges of the parameters considered. The result shows these effects as η approaches 0.4. The slab surface dimensionless temperature (and the thermal profiles) continue to increase at a successively smaller increment as time increases, indicating the approach of a steady state.

Figure 1b shows the independent variation of variable properties for the 2-s dimensionless temperature distribution. Con-

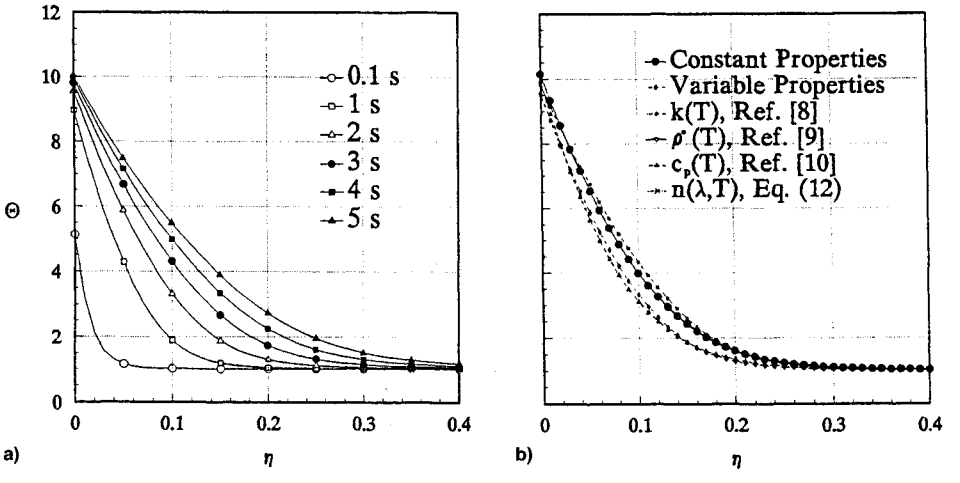

Fig. 1 a) Transient dimensionless temperature vs dimensionless position and b) transient temperature distribution due to thermal and radiative properties, effects at 2 s (T_{aw} = 3715 K, $T_{\infty 1} = T_{\infty 2} = T_0$ = 295 K).

stant properties of $k = 1.4$ W/(m·°C), $\rho = 2200$ kg/m^3, $c_p = 750$ J/(kg·°C), are successively varied as illustrated. Figure 1b shows the effect of this variation of properties from the literature, as noted, at 2 s for Θ as a function of the position. Clearly, specific heat has the largest impact, while refractive index effects are unexpectedly small for this problem.

Figure 2 shows the transient Q^c, normalized with the initial convective surface flux, as a function of the dimensionless position. Time varies from 0.1 to 5 s. Q^c incorporates an energy balance involving the integration of semitransparent wavelengths ($\lambda \leq 4$ μm) that conserve internal and external radiative flux and opaque wavelengths that yield apparent black emission and absorption at different temperatures. The net effect is a lower Q^c due to the energy balance calculation, which is continuous with the interior finite difference determination at the adjacent nodes. The pronounced hump is due to radiative effects as observed in Fig. 3. This decrease in Q^c trends toward a steady state because the conduction heat flux around the first boundary is decreased and the conduction heat flux approaching the second boundary is increased. After reaching a steady state, the gradient of the summation of the conduction and radiation heat flux will be zero.

Figure 3 shows the Q^r, normalized with the initial convective surface flux, as a function of the dimensionless position. Again, time varies from 0.1 to 5 s; note that at 0.1 s the radiation is based on the relatively low temperature, resulting in a very small net radiation flux (almost zero). For later times, more negative radiative flux is out of the slab. The boundary dimensionless net radiative flux varies from very small value initially to increasingly negative values due to the high-temperature surface re-emitting to $T_{\infty 1}$. This trend is expected to continue, since the surface temperature is greater than $T_{\infty 1}$ and increasing with time. Although the highest temperature is always at the first boundary, the highest radiation heat flux is not located at the position of the highest temperature and the peak is moving toward the positive η direction as time is increased. For part of the high-temperature range, the glass is optically thin; as the optical thickness is increased, the radiation heat flux is increased. Since the temperature is decreased so rapidly as η is increased, the radiation heat flux has to decrease after a certain position, creating a peak. As time is increased, temperature effects move deeper into the slab so that the peak is moving toward the positive η direction. The position of the peak corresponds to the position of the hump in Q^c, but the effect on Θ is apparently small as shown on Fig. 1a.

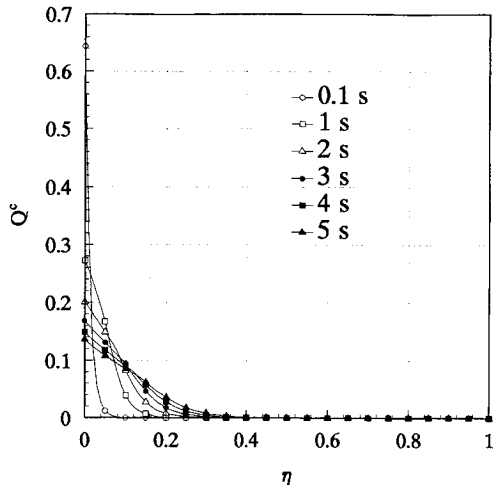

Fig. 2 Transient dimensionless conduction heat flux vs dimensionless position ($T_{aw} = 3715$ K, $T_{\infty 1} = T_{\infty 2} = T_0 = 295$ K).

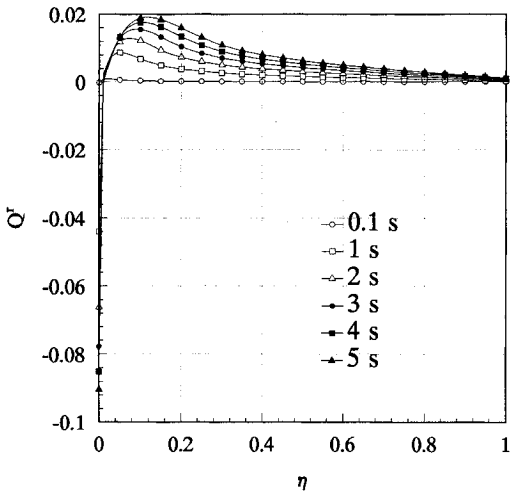

Fig. 3 Transient dimensionless net radiative heat flux vs dimensionless position ($T_{aw} = 3715$ K, $T_{\infty 1} = T_{\infty 2} = T_0 = 295$ K).

In conclusion, a detailed thermal analysis for transient conduction and nongray radiation of glass subjected to high levels of convection is considered. Variation of results due to the best available refractive index data was found to be small. The radiation heat flux creates a peak value that does not coincide with the peak temperature. This effect, in turn, produces a hump in the results for dimensionless conduction heat flux, but has little effect on the temperature distribution. The highest temperature, however, always occurs at the first boundary, which allows the prediction of the onset of softening and subsequent distortion of optics.

Acknowledgments

Special thanks go to B. K. Feather and R. K. Matthews of Calspan Corporation/AEDC Operations for their technical assistance. Special thanks also to J. E. Francis of Bradley University, Peoria, Illinois, for initiating this work.

References

[1]Field, R. E., and Viskanta, R., "Measurement and Prediction of Dynamic Temperatures in Unsymmetric Cooled Glass Windows," *Journal of Thermophysics and Heat Transfer*, Vol. 7, No. 4, 1993, pp. 616–623.

[2]Gardon, R., "A Review of Radiant Heat Transfer in Glass," *Journal of the American Ceramic Society*, Vol. 44, No. 7, 1961, pp. 305–312.

[3]Sutton, W. H., "A Short Time Solution for Coupled Conduction and Radiation in a Participating Slab Geometry," *Journal of Heat Transfer*, Vol. 108, No. 2, 1986, pp. 465–466.

[4]Su, M. H., "High Temperature Heat Transfer in Semitransparent Materials," Ph.D. Dissertation, Univ. of Oklahoma, Norman, OK, 1993.

[5]Hornbeck, R. W., *Numerical Methods*, Prentice–Hall/Quantum Publishers, Englewood Cliffs, NJ, 1975.

[6]Siegel, R., and Howell, J. R., *Thermal Radiation Heat Transfer*, McGraw–Hill, New York, 1972.

[7]Touloukian, Y. S., *Thermophysical Properties of High Temperature Solid Material*, Vol. 4, Pt. II, Thermophysical Properties Research Center, Purdue Univ., West Lafayette, IN, Macmillan, New York, 1967.

[8]Wray, K. L., and Connolly, T. J., "Thermal Conductivity of Fused Silica at High Temperature," *Journal of Applied Physics*, Vol. 30, No. 11, 1959, pp. 1702–1705.

[9]Bacon, J. F., Hasapis, A. A., and Wholley, J. W., "Viscosity and Density of Molten Silica and High Silica Contest Glasses," *Physics and Chemistry of Glasses*, Vol. 1, No. 3, 1960, pp. 90–98.

[10]Kelley, K. K., "High Temperature Heat Content, Heat Capacity and Entropy Data for Inorganic Compounds," U.S. Bureau of Mines, Bulletin 584, Washington, DC, 1960.

[11]Malitson, I. H., "Interspecimen Comparison of the Refractive Index of Fused Silica," *Journal of the Optical Society of America*, Vol. 55, No. 10, 1965, pp. 1205–1209.

[12]Wray, J. H., and Neu, J. T., "Refractive Index of Several Glasses as a Function of Wavelength and Temperature," *Journal of the Optical Society of America*, Vol. 59, No. 6, 1969, pp. 774–776.
[13]Modest, M. F., *Radiative Heat Transfer*, McGraw–Hill, New York, 1993, p. 104.

Transient Emittance Limit for Cooling a Semitransparent Radiating Layer

Robert Siegel*
NASA Lewis Research Center, Cleveland, Ohio 44135

Nomenclature

a	=	absorption coefficient of layer, m^{-1}
c	=	specific heat of radiating medium, $W \cdot s/kg \cdot K$
D	=	thickness of radiating layer, m
E_1, E_2, E_3	=	exponential integral functions
$F(X)$	=	shape of temperature distribution in product solution
n	=	refractive index of layer
q	=	heat flux, W/m^2
$\tilde{q}$	=	$q/\sigma T_{ref}^4$
q_0	=	outgoing flux, W/m^2
T	=	absolute temperature, K
T_{ref}	=	arbitrary reference temperature, K
T_m	=	integrated mean layer temperature, K
t	=	T/T_{ref}
t_m	=	T_m/T_{ref}
X	=	x/D
x	=	coordinate in direction across layer, m
ε_{fd}	=	"fully developed" transient emittance of layer
ε_{ut}	=	emittance of a layer at uniform temperature
κ_D	=	optical thickness of layer, aD
ρ	=	density of radiating medium, kg/m^3
ρ'	=	internal reflectivity at a boundary
σ	=	Stefan–Boltzmann constant, $W/m^2 \cdot K^4$
τ	=	dimensionless time, $(4\sigma T_{ref}^3/\rho c D)$(time)

Introduction

THIS note will show a special feature of transient radiative cooling of a plane layer in the limit of zero heat conduction. The refractive index of the layer is larger than one, and so the layer has internal reflections from its boundaries that are assumed diffuse. The layer is cooling in lower temperature surroundings, and so externally incident radiation is negligible. The transient emittance is the instantaneous radiative flux leaving one side of the layer divided by the blackbody flux corresponding to the layer instantaneous mean temperature. A limit is found where this emittance becomes constant for each optical thickness and refractive index of the layer. The emittance becomes constant, although the heat loss, mean temperature, and temperature distribution are all changing with time.

Received Sept. 28, 1994; revision received Oct. 21, 1994; accepted for publication Oct. 24, 1994.

*Senior Research Scientist, Research Academy. Fellow AIAA.

Transient cooling of a plane layer with $n > 1$ in cold vacuum surroundings was calculated in Ref. 1 with an implicit finite difference procedure. After an initial transient period, the transient emittance became constant for each set of parameters in the limit of zero heat conduction in the layer. This had been shown in Refs. 2 and 3 for a plane layer and a two-dimensional rectangular solid with $n = 1$. This Note will show that a transient similarity solution exists when $n > 1$, which produces reflections within the layer. Fully developed emittance values ε_{fd} are evaluated from the similarity solution and are compared with values for a layer at uniform temperature. From the behavior of the transient solutions in Ref. 1 the ε_{fd} provide a lower emittance limit during transient cooling for the conditions considered here. The shape of the temperature distribution in the fully developed similarity region is found to be rather insensitive to both refractive index and optical thickness.

Analysis

A plane layer extending from $x = 0$ to $x = D$ is a gray-emitting, absorbing, and nonscattering medium with $n > 1$; heat conduction is small and is neglected. The layer is initially at uniform temperature and is placed in much cooler vacuum surroundings, and so energy is lost only by radiation. The surrounding temperature is low enough that radiation from the surroundings to the layer can be neglected.

The transient energy equation in dimensionless form is[1]

$$\frac{\partial t}{\partial \tau} = -n^2\kappa_D t^4(X,\tau) + \frac{\kappa_D}{2}\left(\tilde{q}_0(\tau)\{E_2(\kappa_D X) + E_2[\kappa_D(1 - X)]\} + n^2\kappa_D\int_0^1 t^4(X^*,\tau)E_1(\kappa_D|X^* - X|)\,dX^*\right) \quad (1)$$

Properties are assumed independent of temperature. The $\tilde{q}_0$ is the diffuse flux directed into the layer that is leaving either boundary by reflection. The $\tilde{q}_0$ was obtained in terms of t^4 in Ref. 4, where steady temperatures were calculated for a heated layer with $n > 1$:

$$\tilde{q}_0(\tau) = \frac{2n^2\rho'\kappa_D\int_0^1 t^4(X,\tau)E_2(\kappa_D X)\,dX}{1 - 2\rho' E_3(\kappa_D)} \quad (2)$$

A product solution is now tried: $t(X,\tau) = t(0,\tau)F(X)$, where $F(0) = 1$. The $F(X)$ is the shape of the transient temperature distribution; the success of the product solution shows that $F(X)$ remains fixed in the transient region being analyzed. The $t(1,\tau) - t(0,\tau) = t(0,\tau)[F(1) - 1]$ is the amplitude of the temperature distribution that changes with time as the layer cools. The product solution is substituted into Eq. (1) combined with Eq. (2) and the variables are separated to yield:

$$\frac{1}{t^4(0,\tau)}\frac{dt(0,\tau)}{d\tau} = -\frac{n^2\kappa_D}{F(X)}F^4(X) + \frac{\kappa_D}{2F(X)}\left\{2n^2\rho'\kappa_D\frac{E_2(\kappa_D X) + E_2[\kappa_D(1 - X)]}{1 - 2\rho' E_3(\kappa_D)} \times \int_0^1 F^4(X)E_2(\kappa_D X)\,dX + n^2\kappa_D\int_0^1 F^4(X^*)E_1(\kappa_D|X^* - X|)\,dX^*\right\} \quad (3)$$

With the variables separated, each side of Eq. (3) must be a constant. A convenient expression for the constant is to use the right side of Eq. (3) at $X = 0$, noting that $F(0) = 1$. The